Simultaneous Quantification of the Concentration and Carbon Isotopologue Distribution of Polar Metabolites in a Single Analysis by Gas Chromatography and Mass Spectrometry

Evers, Bernard; Gerding, Albert; Boer, Theo; Heiner-Fokkema, M. Rebecca; Jalving, Mathilde; Wahl, S. Aljoscha; Reijngoud, Dirk Jan; Bakker, Barbara M.

DOI
10.1021/acs.analchem.1c01040

Publication date
2021

Document Version
Final published version

Published in
Analytical Chemistry

Citation (APA)
Evers, B., Gerding, A., Boer, T., Heiner-Fokkema, M. R., Jalving, M., Wahl, S. A., Reijngoud, D. J., & Bakker, B. M. (2021). Simultaneous Quantification of the Concentration and Carbon Isotopologue Distribution of Polar Metabolites in a Single Analysis by Gas Chromatography and Mass Spectrometry. *Analytical Chemistry*, *93*(23), 8248-8256. https://doi.org/10.1021/acs.analchem.1c01040

analytical chemistry

pubs.acs.org/ac

Article

Simultaneous Quantification of the Concentration and Carbon Isotopologue Distribution of Polar Metabolites in a Single Analysis by Gas Chromatography and Mass Spectrometry

Bernard Evers, Albert Gerding, Theo Boer, M. Rebecca Heiner-Fokkema, Mathilde Jalving, S. Aljoscha Wahl, Dirk-Jan Reijngoud, and Barbara M. Bakker*

Cite This: *Anal. Chem.* 2021, 93, 8248−8256

Read Online

ACCESS | Metrics & More | Article Recommendations | Supporting Information

ABSTRACT: ^{13}C-isotope tracing is a frequently employed approach to study metabolic pathway activity. When combined with the subsequent quantification of absolute metabolite concentrations, this enables detailed characterization of the metabolome in biological specimens and facilitates computational time-resolved flux quantification. Classically, a ^{13}C-isotopically labeled sample is required to quantify ^{13}C-isotope enrichments and a second unlabeled sample for the quantification of metabolite concentrations. The rationale for a second unlabeled sample is that the current methods for metabolite quantification rely mostly on isotope dilution mass spectrometry (IDMS) and thus isotopically labeled internal standards are added to the unlabeled sample. This excludes the absolute quantification of metabolite concentrations in ^{13}C-isotopically labeled samples. To address this issue, we have developed and validated a new strategy using an unlabeled internal standard to simultaneously quantify metabolite concentrations and ^{13}C-isotope enrichments in a single ^{13}C-labeled sample based on gas chromatography−mass spectrometry (GC/MS). The method was optimized for amino acids and citric acid cycle intermediates and was shown to have high analytical precision and accuracy. Metabolite concentrations could be quantified in small tissue samples (≥20 mg). Also, we applied the method on ^{13}C-isotopically labeled mammalian cells treated with and without a metabolic inhibitor. We proved that we can quantify absolute metabolite concentrations and ^{13}C-isotope enrichments in a single ^{13}C-isotopically labeled sample.

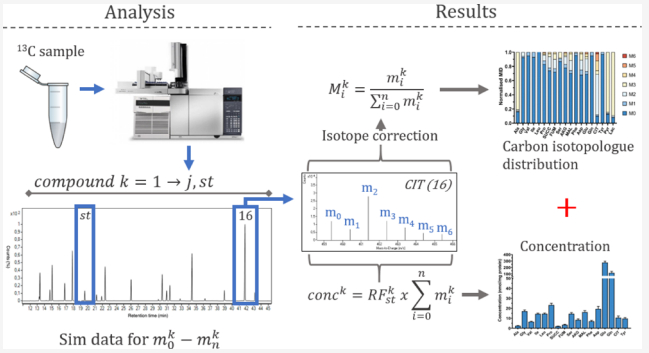

Unravelling the properties of complex metabolic networks has a long-standing history in biotechnology, bioengineering, and (bio)medical sciences.[1−8] In recent years, advances in analytical chemistry and computational modeling have paved the way for novel approaches to quantify metabolic changes in biochemical networks in various specimens.[9−12] With the introduction of metabolomics, absolute or relative changes in metabolite concentrations can be quantified, enabling detailed characterization of the metabolome in biological specimens.[13] However, the rate and direction of these changes (i.e., flux), which characterize the metabolic phenotype and reveal the pathway activities, cannot be readily inferred solely from measuring the absolute or relative metabolite concentrations.[14,15] Therefore, for a more detailed analysis of cellular metabolism, the use of stable-isotope-labeled tracers has been introduced. The frequently employed ^{13}C-isotopically labeled substrates have proven their value in studying the metabolic pathway activity, vulnerability, and regulation in various specimens, including the analysis of needle biopsies in human in vivo ^{13}C-tracer studies.[6,16,17] Combining the absolute concentrations and ^{13}C-isotope tracing with subsequent extracellular flux measurements would facilitate computationally time-resolved flux quantification.[18−22]

Mass spectrometry (MS) and tandem mass spectrometry (MS/MS) coupled to a liquid (LC) or gas chromatography (GC) are currently the preferred analytical techniques for the quantification of a broad spectrum of absolute metabolite concentrations and sensitive measurements of ^{13}C-isotope enrichments in small biological samples.[15,23−25] Classically, two samples are needed for the quantification of ^{13}C-isotope enrichments and absolute metabolite concentrations. The first sample containing ^{13}C-labeled metabolites is used to quantify ^{13}C-isotope enrichments and a separate unlabeled sample is

Received: March 9, 2021
Accepted: May 24, 2021
Published: June 1, 2021

https://doi.org/10.1021/acs.analchem.1c01040
Anal. Chem. 2021, 93, 8248−8256

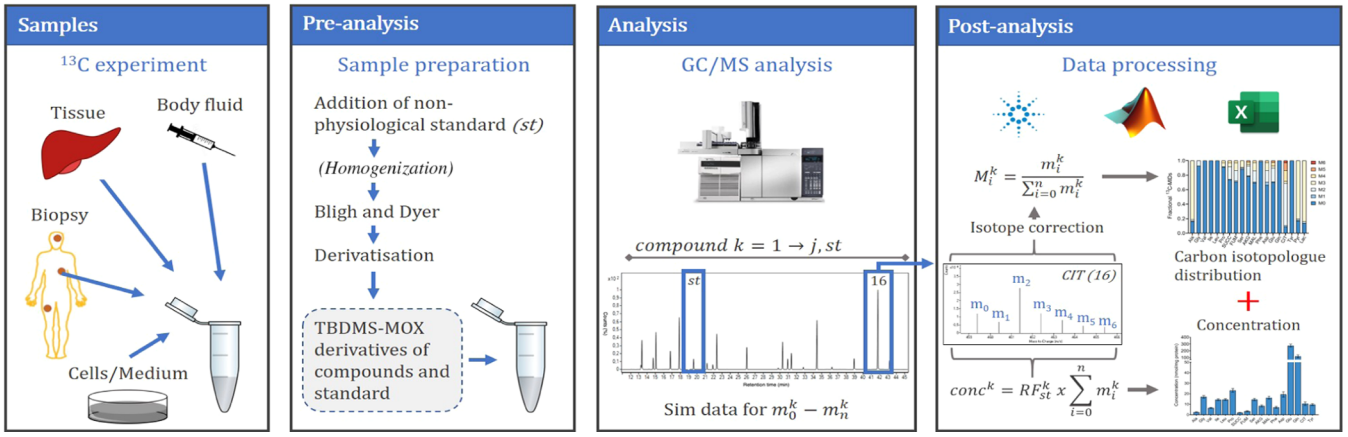

Figure 1. Simultaneous quantification of the carbon isotopologue distribution and absolute concentration of polar metabolites in various ^{13}C-labeled samples. The response factor (RF) of the calibration standard for each metabolite is used to quantify the absolute metabolite concentration in ^{13}C-labeled samples.

prepared for the quantification of absolute metabolite concentrations. The unlabeled sample is required for the quantification of absolute metabolite concentrations since current methods rely mostly on isotope dilution mass spectrometry (IDMS).[26−29] For IDMS, the absolute metabolite concentrations are quantified using a stable isotopically labeled analogue of the metabolite of interest as the internal standard. The labeled internal standard is then added to calibration standards and unlabeled samples for subsequent analysis of the absolute metabolite concentrations. In MS analyses, the isotopologues of the labeled internal standard and the metabolite of interest are selected based on, e.g., intensity or specificity, and their intensities are measured. This approach works well for the absolute quantification of unlabeled metabolites. It is, however, not suitable when stable-isotope labeled tracers are applied since the addition of a labeled internal standard would hamper the determination of the isotopologue spectrum of the selected fragment of the labeled metabolite of interest. This is of particular importance in in vivo ^{13}C-tracer studies, where unique patient samples are analyzed. It would, therefore, have great implications for a detailed analysis of cellular metabolism if simultaneous quantification of the absolute metabolite concentrations and ^{13}C-isotope enrichments can be performed in a single ^{13}C-isotopically labeled sample. To this end, Heuillet et al. have recently described such a method for the simultaneous analysis of amino acid concentrations and ^{13}C-isotope incorporation using an LC-MS-based method.[30] Here, doubly labeled analogues of the metabolites of interest are used as internal standards and prepared from ^{15}N^{13}C-labeled cell extracts from *Escherichia coli*. The advantage of a double isotopically labeled internal standard is, that it can be resolved from the isotopologue spectrum of a single isotopically labeled metabolite of interest and therefore applicable to quantify both absolute concentrations and isotope incorporations. The preparation of these doubly labeled cell extracts, however, remains laborious, and in its current form, the method is only applicable to nitrogen-containing metabolites, such as amino acids. For broader applicability, we have developed a GC/MS method based on an unlabeled internal standard, norleucine (Nle), and demonstrate its feasibility to simultaneously quantify the absolute metabolite concentrations and ^{13}C-isotope enrichments in a single analysis (Figure 1). The fundamental assumption in metabolic tracer studies is the equal engagement of labeled and unlabeled metabolites in metabolism. Therefore, the concentration of the metabolite in the ^{13}C-labeled sample, comprising both labeled and unlabeled metabolite, is the sum of the contributions of all isotopologues of that metabolite, irrespective of the degree of labeling. Usually, in IDMS, the intensity of the isotopologues with the highest intensities, m_0 of the metabolite and m_i of the added $^{13}C_i$-labeled internal standard, is used to quantify the absolute metabolite concentration. When, however, the full isotopologue spectrum of the metabolite is used and an unlabeled internal standard is added to the sample, the absolute concentration of the metabolite can be determined with high accuracy and sensitivity independent of the label distribution over the isotopologues of a selected fragment. At the same time, the carbon isotopologue distribution (CID) of the metabolite of interest can be obtained. The method was optimized for the citric acid cycle (CAC) intermediates and amino acids. Subsequently, we demonstrated the applicability and validation of the GC/MS method for the quantification of metabolites of interest in mammalian cells and small human tissue samples. Finally, in a proof-of-concept experiment, we show the simultaneous quantification of the ^{13}C-isotope enrichments and absolute metabolite concentrations in mammalian cells in an experiment in which [U-^{13}C]glucose was added.

EXPERIMENTAL SECTION

GC/MS Sample Preparation. The samples (900 μL) for GC/MS analysis were thawed on ice, followed by the addition of 50 μL of the internal standard Nle (0.4 mM in Milli-Q water) to each sample. The samples were delipidated and deproteinated according to the Bligh and Dyer procedure.[31] Briefly, the samples were transferred to a glass tube and mixed with 1 mL of ice-cold Milli-Q water and 1 mL of ice-cold methanol. Subsequently, 2 mL of ice-cold chloroform was added. Glass tubes were closed with a screw cap and vortexed for 30 min at 4 °C, followed by centrifugation for 10 min at 2500*g* at 4 °C. Centrifugation produced a biphasic separation in which the polar metabolites are in the upper methanol-Milli-Q water phase and proteins are in the interphase. The upper phase was transferred to a clean derivatization tube (Wheaton) and dried under a stream of nitrogen at 37 °C. The dried polar

https://doi.org/10.1021/acs.analchem.1c01040
Anal. Chem. 2021, 93, 8248−8256

Table 1. Quantification of CAC Intermediates and Amino Acids and Method Performance by GC/MS

				precision CV (%)		recovery (n = 10)[a]	
metabolite	RT (min)	range (nmol)	linearity (R^2)	repeatability (n = 10)	intermediate precision (n = 3)	mean (%)	CV (%)
Ala	13.40	5−100	1.000	0.7	0.5	102.3	2.2
Gly	14.80	5−100	1.000	2.9	0.8	100.7	4.6
Val	16.80	5−100	1.000	0.3	0.5	100.5	2.5
Ile	17.80	5−100	1.000	0.3	0.3	100.3	2.7
Leu	19.00	5−100	1.000	0.3	0.4	99.6	2.7
Pro	21.00	5−50	0.991	0.1	0.3	82.3	16.2
SUCC	21.90	1−20	0.999	0.7	0.8	105.6	6.0
FUM	22.40	5−100	0.999	0.8	0.6	100.4	7.1
Ser	26.00	5−100	1.000	0.4	2.0	96.4	4.5
AKG	29.80	0.5−10.5	0.998	1.4	1.5	112.9	10.8
MAL	30.30	7.5−150	0.996	1.2	0.6	106.2	6.0
Phe	30.90	5−100	0.999	0.8	1.8	97.4	3.1
Asp	31.40	5−100	0.998	1.0	3.7	95.2	8.3
Glu	34.40	10−200	0.999	0.6	1.8	95.4	9.2
Gln	39.10	40−400	0.999	2.0	0.4	98.1	12.6
CIT	41.80	10−200	0.999	3.0	1.8	98.0	6.5
Tyr	43.20	5−100	0.993	3.9	1.7	86.1	3.7

[a]50 μL of amino acids stock and 40 μL of CAC intermediates stock were spiked to human A375 cells and 90 μL of PBS was added to the control human A375 cells (see Table S1, preparation of amino acid and CAC intermediate stock).

metabolites were dissolved in 40 μL of MOX in pyridine solution (20 mg mL^{-1}) and incubated for 90 min at 37 °C. The samples were silylated for 1 h at 55 °C by adding 60 μL of MTBSTFA with 1% TBDMS-Cl. The resulting MOX-TBDMS derivatives were centrifuged at ambient temperature for 10 min at 1250g. The clear supernatant was transferred to a 1.5 mL GC/MS vial with a 0.1 mL microinsert (APG Europe, Netherlands) and subjected to GC/MS analysis. Calibration standards (900 μL) for CAC intermediates and amino acids were treated in parallel in an identical manner (Table S1).

GC/MS Acquisition. GC/MS measurements were carried out on Agilent 7890A GC coupled to an Agilent 5975C Quadrupole MS, equipped with a CTC Analytics PAL autosampler (CTC Analytics AG, Switzerland). One microliter of the sample was injected on an Agilent DB-35ms column (30 m × 250 μm internal diameter, 0.25 mm film thickness) in split mode with a ratio of 1:20. Single taper glass liners with glass wool were used (Agilent). The inlet temperature was 280 °C and the helium split flow of 20 mL min^{-1} was applied. Carrier gas (helium) flow during the analysis was set at 1 mL min^{-1}. The GC oven temperature was held at 100 °C for 3 min and then raised by 3.5 °C min^{-1} up to 300 °C with a 1 min hold time. The temperature of the transfer line was set at 300 °C, the MS source at 230 °C, and the quadrupole at 150 °C. The electron ionization (EI) source was fixed at 70 eV and polar metabolites were measured as their $[M\text{-}57]^+$ fragments in selective-ion-monitoring (SIM) mode. Isotopologue spectra ($m_0 - m_i$) at nominal mass resolution were monitored for each metabolite except for Nle. For Nle, the isotopologue m_0 was monitored (for m/z values monitored, see Table S2).

GC/MS Data Processing. Peak areas of $m_0 - m_i$ isotopologues of the $[M\text{-}57]^+$ fragment of each metabolite of interest and m_0 of the $[M\text{-}57]^+$ fragment of Nle were integrated using MassHunter Quantitative Analysis software for MS (version B.07.00, Agilent). The measured isotopologues of each metabolite of interest were corrected for naturally occurring isotopes in a two-step procedure. The first correction step was done according to Wahl et al.[32] This step corrects for all-natural isotopes of the chemical derivatives and the metabolite of interest, except for the carbon atoms in the core metabolite. Therefore, an additional correction was applied to correct for the natural abundance of ^{13}C in the carbon skeleton of metabolites of interest, retrieving the CIDs that originate from the ^{13}C-tracer only (for details, see Method S1). Separately, the same data set of integrated peak areas ($m_0 - m_i$) was used to calculate the absolute metabolite concentrations in the ^{13}C-isotopically labeled and unlabeled samples. For this quantitative approach, the individual peak areas within the $m_0 - m_i$ spectrum of the fragment of each metabolite were summed up and divided by the m_0 peak area of Nle to calculate the metabolite to the internal standard ratio for the samples and calibration standards. To obtain a calibration curve, the ratios for the calibration standards were plotted for each metabolite against the known amount of the respective metabolite. Subsequently, a linear regression model was applied to be able to calculate the amount of metabolites in the samples. The amount of metabolites in the cell samples was corrected for the total cell protein content and corrected for wet weight in the case of tumor tissue homogenates.

Statistical Analysis. Statistical analysis and data visualization were performed in Prism 8 (GraphPad Software, Inc., CA). The type of statistical test with the corresponding P value and the number of replicates (n) are reported in the legend of the respective figures.

Further details on the experimental procedures and analyses can be found in Methods S1−S11 (Supporting Information).

RESULTS AND DISCUSSION

Method Performance. *Methodology.* For a targeted analysis of the CAC intermediates and amino acids, the retention times and ion fragmentation patterns of pure standards were determined (see Table 1 for metabolites of interest). Metabolite identification was performed under electron ionization (EI) and the ion fragmentation pattern of each analyte was compared to a NIST reference ion fragmentation pattern. Upon EI, TBDMS-derivatized, Lac, Pyr, CAC intermediates, and amino acids yielded strong $[M\text{-}57]^+$ fragments, i.e., fragments that had lost a t-butyl (m/z =

https://doi.org/10.1021/acs.analchem.1c01040
Anal. Chem. 2021, 93, 8248−8256

57) from the TBDMS group.[33−36] The respective $[M-57]^+$ fragment of each analyte was used in the SIM mode for further GC/MS analyses (Table S2). Lac, Pyr, and all CAC intermediates and amino acids of interest are baseline-separated on the GC, including the internal standard Nle (Figures S1 and S2).

Next, the working range for an accurate isotopologue quantification of the metabolites of interest was determined. To this end, human A375 cells, cultured for 8 h on [U-^{13}C]glucose, were pooled and a serial dilution, ranging from 0.03 up to 1.50 mg protein, prepared for GC/MS analysis. Here, CIT is used as an example to indicate that the measured fractional contributions of the isotopologues do not depend on sample dilution between 0.13 and 1.50 mg protein (Figure 2). The other CAC intermediates, and Lac and Pyr, even show a constant response starting as low as 0.06 mg of protein (Figure S3). For the amino acids Val, Ile, Leu, Ser, Phe, and Glu, the response is constant from 0.13 mg, while for Ala, Asp, Tyr, and Gly, Pro, Gln, they are constant from 0.25 and 0.50 mg protein, respectively (Figure S4). Therefore, to include all metabolites of interest for isotopologue quantification, a minimum of 0.50 mg protein is advised. The repeatability of isotopologue quantification by the analytical method was acceptable with a coefficient of variation (CV) <10.88% for all isotopologues from the metabolites of interest having a fractional contribution of >0.03% (Table S3).

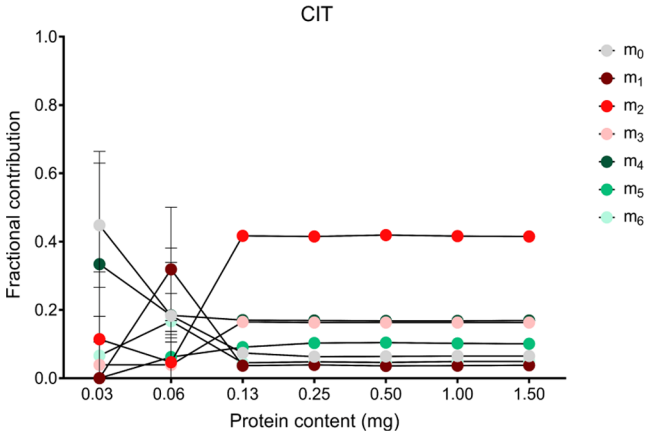

Figure 2. Working range for isotopologue quantification of CIT in human A375 cells cultured in the presence of [U-^{13}C]glucose for 8 h. The isotopologue spectrum, $m_0 - m_i$, as depicted, is not corrected for natural abundance. The fractional contribution of each isotopologue is presented as mean ± standard deviation (SD) (n = 3 technical replicates).

In contrast to IDMS methods, which quantify the absolute metabolite concentrations using ^{13}C-isotopically labeled internal standards, our method has been designed to quantify absolute metabolite concentrations with a single unlabeled internal standard. The unlabeled internal standard Nle was added to the sample of interest and calibration standards followed by GC/MS analysis. The acquired calibration curves for the metabolites of interest were linear over a variable range of 0.5-400 nmol (Figure S5) with a good (R^2 > 0.991) up to excellent (R^2 = 1.000) correlation coefficient, depending on the analyte (Table 1). The absolute quantification of Lac and Pyr concentrations by GC/MS was below the limit of quantification (LOQ) with a signal-to-noise ratio (SNR) below 10 (data not shown). Therefore, enzymatic assays were applied for the absolute quantification of Lac and Pyr concentrations (LOQ of 0.10 and 0.05 nmol, respectively). The repeatability of the analytical method after 10 consecutive measurements of standard mixture S4 (Table S1) was excellent with a CV <3.9% for all metabolites (Table 1). The intermediate precision based on three consecutive measurements of the same standard mixture S4 on three different days had a similar low CV (<3.7% for all metabolites; Table 1), demonstrating a high day-to-day precision of GC/MS analyses and stability of derivatized metabolites at room temperature. Finally, the absolute quantification of amino acid concentrations by GC/MS showed excellent agreement to those of the widely used

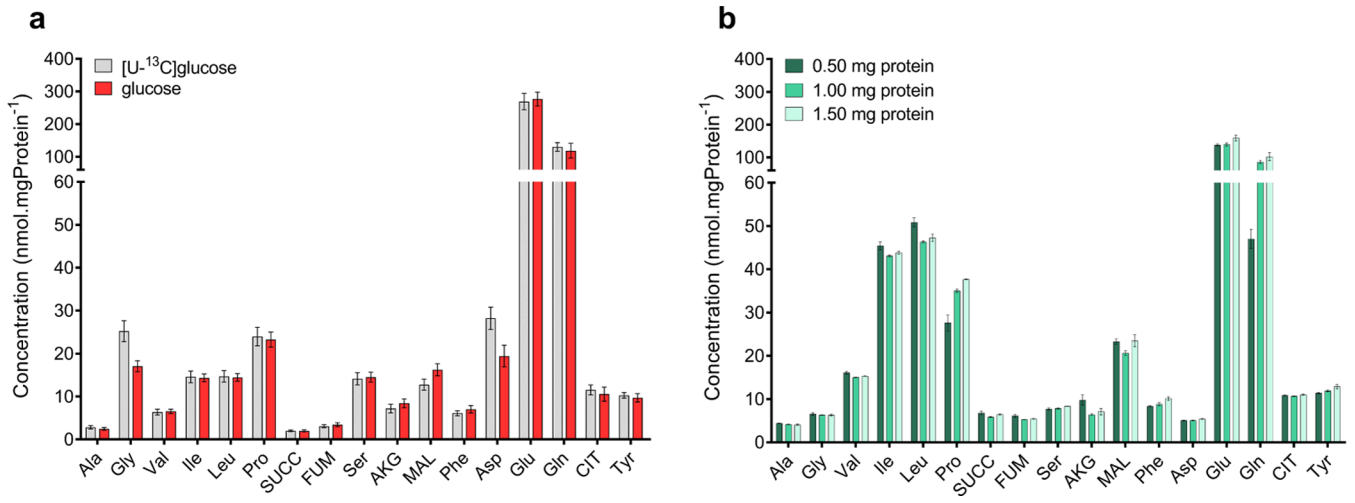

Figure 3. Validation of the quantification of CAC intermediates and amino acid concentrations in ^{13}C-labeled samples. (a) Comparison of the quantification of CAC intermediates and amino acids in extracts of human A375 cells cultured in the presence of [U-^{13}C]glucose or unlabeled glucose. Mean concentrations ± standard error of the mean (SEM) of the metabolites of interest are corrected for the total amount of protein (n = 6 biological replicates). P > 0.05 comparing [U-^{13}C]glucose with unlabeled glucose. (b) Working range for the quantification of CAC intermediates and amino acid concentrations in human A375 cells cultured in the presence of [U-^{13}C]glucose for 8 h (mean ± SD, n = 3 technical replicates). P > 0.05 comparing 0.50, 1.00, and 1.50 mg sample sizes to each other (see Figure S6 for the full sample size range). P values were calculated using multiple t-tests (a) and a two-way analysis of variance (ANOVA) (b) with a Holm−Šídák correction for multiple comparisons.

https://doi.org/10.1021/acs.analchem.1c01040
Anal. Chem. 2021, 93, 8248−8256

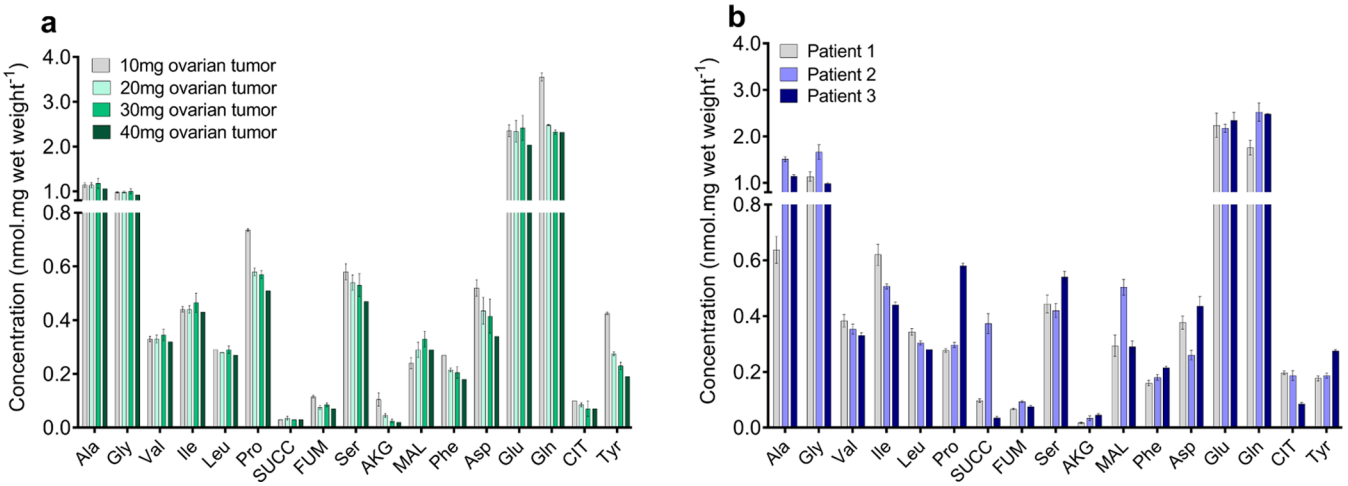

Figure 4. Absolute quantification of CAC intermediates and amino acids in small tumor tissue samples. (a) Quantification of metabolite concentrations in increasing sample size of ovarian tumor tissue normalized to wet weight (mean ± SD, n = 2 technical replicates, except for 40 mg, n = 1). (b) Metabolite concentration profile in ovarian tumor tissue of three patients normalized to wet weight (mean ± SD, n = 3 technical replicates, except for patient 3, n = 2).

and validated Biochrom 30+ method for amino acid analyses (Figure S6).[37] Subsequently, the percentage recovery in a biological matrix was determined by spiking a known analyte concentration to human A375 cells, measuring the absolute concentration increase in the sample, and comparing this to a standard with the same absolute concentration without the cells. The average recovery yield for each analyte (except Pro, AKG, and Tyr) ranged from 95.2 to 106.2% with a CV lower than 12.6% (Table 1). Pro and Tyr had lower recoveries of 82.3 and 86.1% with a CV of 16.2 and 3.7%, respectively (Table 1). The recovery of AKG was 112.9% with a CV of 10.8%. The recoveries of Pro, Tyr, and AKG were within the acceptable 80−120% range with a CV lower than 15%. Finally, the possibility of interfering compounds in a biological matrix was evaluated by spiking a known amount of CAC intermediates and amino acids to human A375 cells. The calibration curves were shifted relative to the Y-axis due to the presence of an increasing amount of the analyte of interest in the sample, but the slopes were unchanged (Figure S5). This indicates that the sample preparation and GC/MS analysis were not affected by the biological matrix. In conclusion, the GC/MS analysis proved to be reliable for the accurate quantification of isotopologues and absolute metabolite concentrations of CAC intermediates and amino acids.

Validation. We investigated whether the new GC/MS acquisition and data processing results in accurate absolute quantification of metabolite concentrations independent of ^{13}C-isotope enrichment in ^{13}C-labeled samples. To this end, the cells were cultured with uniformly labeled [U-^{13}C]glucose or unlabeled glucose under otherwise identical conditions. The absolute quantification was based on the summation of the individual peak areas of the $m_0 - m_i$ isotopologue spectrum of the metabolite fragments combined with nonlabeled calibration curves, as mentioned earlier. Absolute concentrations were statistically equal for each metabolite of interest in [U-^{13}C]-glucose compared to unlabeled glucose cultures (Figure 3a). Gly and Asp show lower absolute concentrations in glucose cultures when compared with [U-^{13}C]glucose cultures (Figure 3a), but the difference is not significant (mean difference 8.18 and 8.79 μmol·min^{-1}·mg protein^{-1} with $P > 0.05$ for Gly and Asp, respectively). This validation shows that the GC/MS acquisition and data processing approach can be applied to ^{13}C-labeled biological samples to quantify the absolute metabolite concentrations independent of the degree of labeling. Next, the working range for the accurate determination of the absolute metabolite concentrations was determined using the same serial dilution data set as that used for the determination of the working range of isotopologue quantification. Except for Gln and Pro, all metabolites were reproducibly quantified in ^{13}C-labeled samples of human A375 cells from 0.50 mg up to 1.50 mg protein (Figures 3b and S7). A lower limit of 1.00 mg protein is set to accurately quantify the concentrations of Gln and Pro. Therefore, 1.00 mg of protein is minimally required to simultaneously quantify the absolute concentrations and isotopologues of all metabolites of interest. This limit roughly corresponds to the total protein content of human A375 cells cultured on 100 mm culture plates.

Application to Small Tumor Biopsies. Next, we investigated the sensitivity and biological reproducibility of the GC/MS method in small tumor biopsies. First, we estimated the minimal amount of ovarian tumor tissue necessary for an accurate determination of the concentration of the metabolites of interest. Ovarian tumor tissue samples of a single patient ranging from 10 mg up to 40 mg were subjected to GC/MS analysis. All metabolites were reproducibly quantified in human ovarian tumor biopsies samples ranging from 20 mg up to 40 mg (Figure 4a). In 10 mg samples, a subset of metabolites, comprising Pro, FUM, AKG, Gln, and Tyr, was overestimated (Figure 4a). Therefore, these data suggest a lower limit of 20 mg tissue for the quantification of Pro, FUM, AKG, Gln, and Tyr in ovarian tumor tissue. This makes the method applicable to an average needle biopsy (~20 mg). Second, we tested for intratumor variation. Tumor tissue from three patients was divided into three separate pieces and subjected separately to GC/MS analysis. An average CV lower than 13% for all metabolites between different pieces of the same biopsy suggested that the intratumor variation for metabolite concentrations is relatively small in this specific case (Figure 4b and Table S4). Third, we tested the patient-to-patient variation in ovarian tumor tissues from three individual patients. We found that the patient-to-patient variation was

https://doi.org/10.1021/acs.analchem.1c01040
Anal. Chem. 2021, 93, 8248−8256

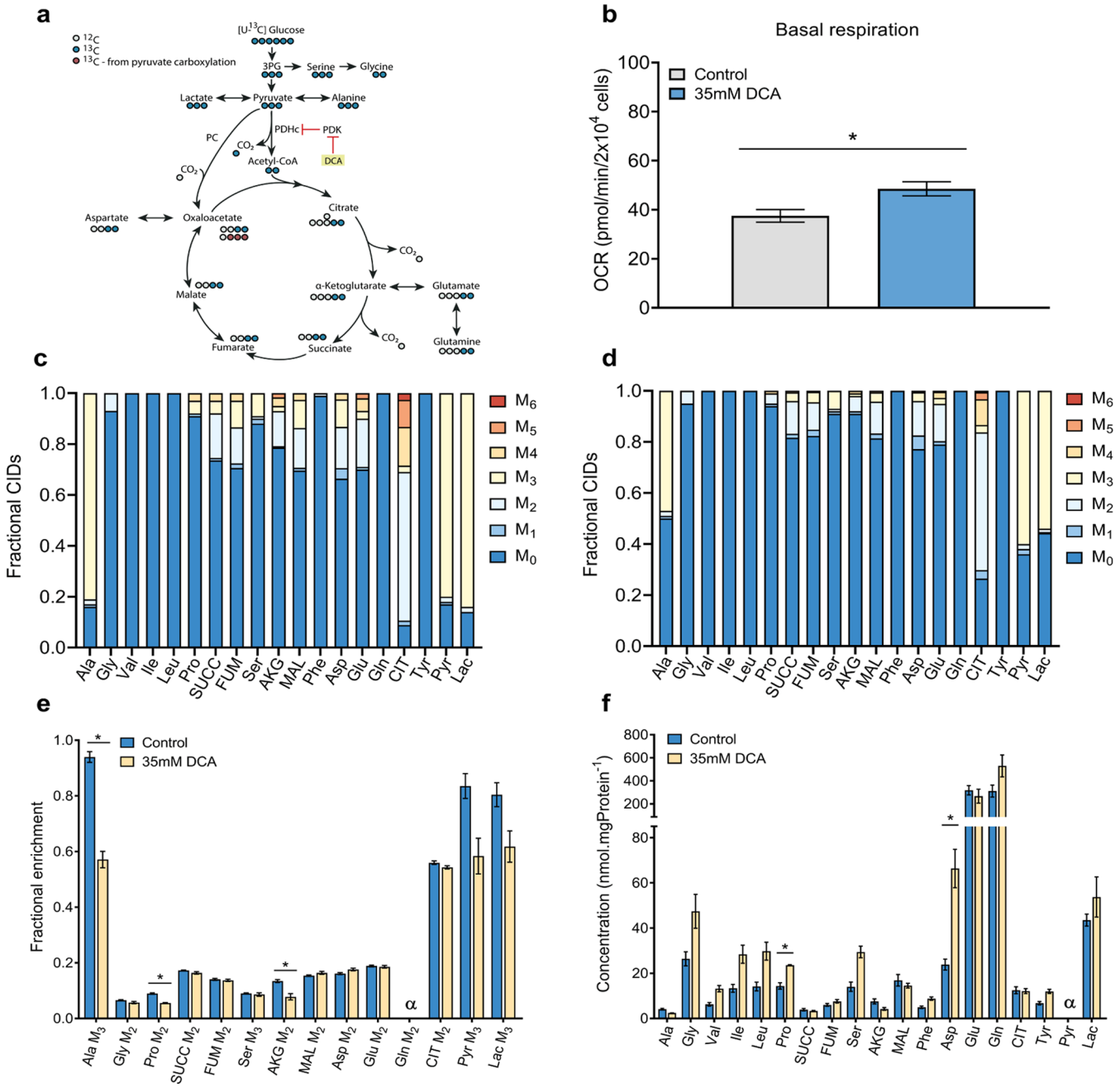

Figure 5. Simultaneous quantification of ^{13}C-isotope labeling and absolute concentrations of CAC intermediates and amino acids in human A375 cells cultured in the presence of [U-^{13}C]glucose. (a) Schematic representation of carbon atom (circles) transitions upon [U-^{13}C]glucose infusion. Isotope label distribution of [U-^{13}C]pyruvate from [U-^{13}C]glucose through glycolysis by pyruvate dehydrogenase in the first turn of the CAC are depicted by blue circles. Red circles indicate the isotope label incorporation from [U-^{13}C]pyruvate from [U-^{13}C]glucose by pyruvate carboxylase (PC). (b) Basal respiration, oxygen consumption rate (OCR), measured in human A375 cells untreated and treated with 35 mM DCA (mean ± SEM, n = 4 biological replicates). (c and d) Fractional ^{13}C-MIDs of the carbon skeleton of metabolites of interest after 8 h [U-^{13}C]glucose uptake for control (c) and 35 mM DCA-treated cells (d) in human A375 cells (mean, n = 4 biological replicates). (e) Fractional ^{13}C-enrichment of most prominent isotopologues of CAC intermediates and amino acids in human A375 cells untreated and treated with 35 mM DCA after 8 h. α, no M2 enrichment in glutamine was detected in all experiments. (f) Metabolite concentration profile of CAC intermediates and amino acids in human A375 cells untreated and treated with 35 mM DCA after 8 h (mean ± SEM, n = 4 biological replicates). Note that the concentrations of Pyr and Lac were estimated based on fluorescent measurements. α, Concentration of Pyr was below the limit of quantification. For (b), (e), and (f), *P < 0.05 comparing 35 mM DCA with control. P values were calculated using a Student's t-test (b) and multiple t-tests with a Holm−Sídák correction for multiple comparisons (e and f).

substantial. Concentrations of Ala, Ile, Pro, SUCC, Ser, Asp, CIT, MAL, and Tyr differed substantially between different patients and were reflected in an average CV of 29% for all metabolites (Figure 4b and Table S4). Together, these data indicate that the GC/MS method is suitable to quantify the absolute metabolite concentrations in needle biopsies. Also, it shows the method's sensitivity to establish patient-specific metabolite profiles in tumor tissue (Figure 4b).

Proof of Concept. As a proof of concept, we aimed to simultaneously quantify the absolute metabolite concentrations

https://doi.org/10.1021/acs.analchem.1c01040
Anal. Chem. 2021, 93, 8248−8256

and ^{13}C-isotope enrichments in a single ^{13}C-labeled sample of human A375 cells treated with dichloroacetate (DCA). DCA is a well-studied metabolic drug that inhibits the enzyme pyruvate dehydrogenase kinase (PDK). Thus, it indirectly activates the conversion of Pyr to acetyl-CoA by the pyruvate dehydrogenase complex (PDHc) (Figure 5a) and redirects Pyr metabolism from lactate production to mitochondrial oxidation.[38,39] Indeed, mitochondrial respiration was increased upon 35 mM DCA treatment in human A375 cells (Figure 5b) and glucose utilization was decreased (Figure S8; 0.073 ± 0.009 and 0.032 ± 0.004 μmol·min^{-1}·mg protein^{-1}; control vs DCA-treated cells, respectively) in the absence of cytotoxicity (Figure S9). Concomitantly, lactate production decreased (0.100 ± 0.014 and 0.045 ± 0.003 μmol·min^{-1}·mg protein^{-1}; control vs DCA-treated cells, respectively) (Figure S8). Contrary to our expectations, the DCA treatment hardly affected the fraction of the glucose influx directed into the lactate production (0.73 ± 0.14 and 0.76 ± 0.14 μmol·min^{-1}·mg protein^{-1} control vs DCA-treated cells, respectively). In this respect, it is important to realize that due to its metabolic effects, DCA evokes growth inhibition in cancer cells, which will affect glucose metabolism in human A375 cells.[39−41]

We expected changes in concentrations and ^{13}C-labeling of glycolytic products, CAC intermediates, and amino acids. Therefore, human A375 cultures preincubated with 35 mM DCA and controls were subjected to [U-^{13}C]glucose isotope tracing experiments and GC/MS analysis. Figure 5a shows a schematic representation of the fate of M6 [U-^{13}C]glucose (six blue dots for 6 ^{13}C). Glycolysis converts M6 glucose into M3 Pyr, M3 Lac, and M3 Ala. Oxidation of Pyr by PDHc results in M2 acetyl-CoA, which is subsequently incorporated into downstream CAC intermediates and amino acids, depicted with two blue dots. Alternatively, Pyr can be converted directly into oxaloacetate via pyruvate carboxylase (PC), leading to M3 CAC intermediates and amino acids depicted with three red dots.

The ^{13}C-isotope enrichment in all metabolites in control and 35 mM DCA-treated cells was calculated as the fractional CIDs of the carbon skeleton of the metabolite of interest with contributions of added ^{13}C-tracer only (Figures 5c,d and S10). As expected, no ^{13}C incorporation was observed into the essential amino acids Ile, Leu, Val, and Phe, nor in Tyr (a direct product of Phe) (Figure 5c,d). Glutamine did not incorporate label either, pointing to a lack of glutamine synthetase in human A375 cells. Thus, these cells can only consume but not produce glutamine. The fractional CIDs of all other metabolites showed incorporation of ^{13}C. For most metabolites, the total incorporation of the ^{13}C label was reduced in the DCA-treated cells compared to control cells (Figure 5c,d). The contributions of specific M2- or M3-labeled fractions were either reduced or unchanged by DCA (Figure 5e). DCA did not affect the absolute concentrations of CAC metabolites, except that of AKG, which was decreased (4.20 ± 0.62 and 7.57 ± 1.13 μmol·min^{-1}·mg protein^{-1}, respectively). However, DCA did cause a trend of increased absolute amino acid concentrations, with Pro and Asp being significantly increased (Figure 5f). Altogether, the GC/MS analysis unveils a clear metabolic rearrangement upon DCA treatment.

Concerning the metabolic interpretation, the reduced M3 isotopologue fractions in Pyr, Ala, and Lac (Figure 5e) are consistent with the decreased uptake of glucose reported above, concomitant with a possible dilution with unlabeled glutamine-derived Pyr via reductive carboxylation. Since the primary effect of DCA is to activate PDHc, we focused on the conversion of M3 Pyr into M2 CIT. M2 CIT itself was not affected by DCA (Figure 5e). However, the fraction M3 Pyr converted to M2 CIT increased by more than 30% upon DCA treatment (0.64 ± 0.03 and 0.95 ± 0.09; control vs DCA-treated cells, respectively). This is consistent with the activation of PDHc by DCA and corresponds to the increased OCR (Figure 5b). The fraction of M3 Pyr converted to M3 CIT via PC did significantly increase upon DCA treatment (0.11 ± 0.01 and 0.06 ± 0.01; DCA-treated cells vs control cells, respectively); however, the respective contribution of PC activity to Pyr metabolism is very low. Interestingly, downstream of CIT, the fraction of M2 label incorporated into AKG is much lower than that of CIT itself. This suggests that extensive label dilution takes place at AKG, most likely by an influx derived from unlabeled glutamine. This dilution was enhanced by the DCA treatment. Finally, the increase of M2 labeling in the downstream CAC metabolites relative to that of AKG indicates that conversion of CIT into downstream CAC metabolites bypasses AKG in part. This may be explained by the conversion of citrate in the cytosol by the consecutive action of ATP-citrate lyase, malate dehydrogenase, and fumarase in DCA-treated cells. The trend of the increased absolute amino acid concentrations (Figure 5f) is consistent with the observed growth inhibition by DCA, which reduces the incorporation of amino acids into biomass. In addition, the oxidation of amino acids may be reduced by DCA. This would be in line with the observations of decreased oxidation of branched-chain amino acids upon DCA treatment in skeletal muscle, although one should be careful to apply these results to A375 cells.[42,43]

CONCLUSIONS

Here, we describe the development of a new strategy using an unlabeled internal standard to simultaneously quantify the absolute concentrations and ^{13}C-isotope distributions of CAC intermediates and amino acids in cell samples starting at 1.00 mg protein based on GC/MS. With this approach, the analysis of the absolute metabolite concentrations becomes independent of the degree of labeling. In addition, the absolute metabolite concentrations can be quantified in tissue samples as small as an average needle biopsy (20 mg), which is highly relevant in preclinical or clinical in vivo settings where the sample size is limited. Using this new strategy, we further show that biologically relevant differences in the absolute metabolite concentrations and ^{13}C-isotope enrichments can be quantified in a single ^{13}C-labeled sample. This feature, of simultaneously quantifying metabolite concentrations and ^{13}C-isotope enrichments using an unlabeled internal standard, may as well apply to other isotopically labeled tracers and metabolites of interest. Also, in the case of in vivo ^{13}C-tracer studies, the application of this method would circumvent the need for separate biopsies to quantify the absolute metabolite concentrations and ^{13}C-isotope enrichments. However, isotopologue quantification in tissue samples needs further validation. It is promising, as shown for the human A375 cells, that the sample size limit for quantification of isotopologues is lower than that of the absolute metabolite concentrations; therefore, we are optimistic that isotopologues can also be quantified in 20 mg tissue samples. We predict that this strategy will have a great impact on future ^{13}C-isotope tracer studies; more specifically, it might increase the information yield in in vivo ^{13}C-tracer studies from a single sample and aid in absolute flux quantification.

https://doi.org/10.1021/acs.analchem.1c01040
Anal. Chem. 2021, 93, 8248−8256

■ ASSOCIATED CONTENT

Supporting Information

The Supporting Information is available free of charge at https://pubs.acs.org/doi/10.1021/acs.analchem.1c01040.

Supporting tables and figures including additional experimental details and methods; preparation of the amino acids stock; preparation of the CAC intermediates stock; and preparation of the standards (PDF)

■ AUTHOR INFORMATION

Corresponding Author

Barbara M. Bakker − *Laboratory of Pediatrics, Section Systems Medicine of Metabolism and Signalling, University of Groningen, University Medical Center Groningen, 9713 AV Groningen, The Netherlands*; Phone: +31 50 361 1542; Email: B.M.Bakker01@umcg.nl

Authors

Bernard Evers − *Laboratory of Pediatrics, Section Systems Medicine of Metabolism and Signalling, University of Groningen, University Medical Center Groningen, 9713 AV Groningen, The Netherlands*; orcid.org/0000-0002-1636-0014

Albert Gerding − *Laboratory of Pediatrics, Section Systems Medicine of Metabolism and Signalling, University of Groningen, University Medical Center Groningen, 9713 AV Groningen, The Netherlands; Laboratory of Metabolic Diseases, Department of Laboratory Medicine, University of Groningen, University Medical Center Groningen, 9700 RB Groningen, The Netherlands*

Theo Boer − *Laboratory of Metabolic Diseases, Department of Laboratory Medicine, University of Groningen, University Medical Center Groningen, 9700 RB Groningen, The Netherlands*

M. Rebecca Heiner-Fokkema − *Laboratory of Metabolic Diseases, Department of Laboratory Medicine, University of Groningen, University Medical Center Groningen, 9700 RB Groningen, The Netherlands*

Mathilde Jalving − *Department of Medical Oncology, University of Groningen, University Medical Center Groningen, 9713 GZ Groningen, The Netherlands*

S. Aljoscha Wahl − *Department of Biotechnology, Applied Science Faculty, Delft University of Technology, 2629 HZ Delft, The Netherlands*

Dirk-Jan Reijngoud − *Laboratory of Pediatrics, Section Systems Medicine of Metabolism and Signalling, University of Groningen, University Medical Center Groningen, 9713 AV Groningen, The Netherlands*

Complete contact information is available at: https://pubs.acs.org/10.1021/acs.analchem.1c01040

Author Contributions

All authors contributed to the writing of the manuscript, and all authors gave their approval to the final version of the manuscript.

Notes

The authors declare no competing financial interest.

■ ACKNOWLEDGMENTS

This work was funded by the UMCG. Furthermore, this study was supported by a Dutch Cancer Society grant awarded to Mathilde Jalving (KWF 10913/2017-1) and a grant from the European Union Horizon 2020 Research and Innovation Program to Barbara Bakker (MESI-STRAT project, grant agreement 754688).

■ REFERENCES

(1) Young, J. D. *Curr. Opin. Biotechnol.* **2013**, *24*, 1108−1115.
(2) Hiller, K.; Metallo, C. M. *Curr. Opin. Biotechnol.* **2013**, *24*, 60−68.
(3) Teusink, B.; Passarge, J.; Reijenga, C. A.; Esgalhado, E.; Van der Weijden, C. C.; Schepper, M.; Walsh, M. C.; Bakker, B. M.; Van Dam, K.; Westerhoff, H. V.; Snoep, J. L. *European Journal of Biochemistry* **2000**, *267*, 5313−5329.
(4) Keibler, M. A.; Fendt, S. M.; Stephanopoulos, G. *Biotechnol. Prog.* **2012**, *28*, 1409−1418.
(5) Metallo, C. M.; Vander Heiden, M. G. *Mol. Cell* **2013**, *49*, 388−398.
(6) Hensley, C. T.; Faubert, B.; Yuan, Q.; Lev-Cohain, N.; Jin, E.; Kim, J.; Jiang, L.; Ko, B.; Skelton, R.; Loudat, L.; Wodzak, M.; Klimko, C.; McMillan, E.; Butt, Y.; Ni, M.; Oliver, D.; Torrealba, J.; Malloy, C. R.; Kernstine, K.; Lenkinski, R. E.; DeBerardinis, R. J. *Cell* **2016**, *164*, 681−694.
(7) Dong, W.; Keibler, M. A.; Stephanopoulos, G. *Metab. Eng.* **2017**, *43*, 113−124.
(8) Puchałka, J.; Oberhardt, M. A.; Godinho, M.; Bielecka, A.; Regenhardt, D.; Timmis, K. N.; Papin, J. A.; Martins Dos Santos, V. A. P. *PLoS Comput. Biol.* **2008**, *4*, No. e1000210.
(9) Antoniewicz, M. R. *Exp. Mol. Med.* **2018**, *50*, 1−13.
(10) Toya, Y.; Shimizu, H. *Biotechnol. Adv.* **2013**, *31*, 818−826.
(11) Vasilakou, E.; Machado, D.; Theorell, A.; Rocha, I.; N??h, K.; Oldiges, M.; Wahl, S. A. *Curr. Opin. Microbiol.* **2016**, *33*, 97−104.
(12) Dai, Z.; Locasale, J. W. *Metab. Eng.* **2016**, *43*, 94−102.
(13) Jang, C.; Chen, L.; Rabinowitz, J. D. *Cell* **2018**, *173*, 822−837.
(14) Sauer, U. *Mol. Syst. Biol.* **2006**, *2*, No. 62.
(15) Jang, C.; Chen, L.; Rabinowitz, J. D. *Cell* **2018**, *173*, 822−837.
(16) Faubert, B.; Li, K. Y.; Cai, L.; Hensley, C. T.; Kim, J.; Zacharias, L. G.; Yang, C.; Do, Q. N.; Doucette, S.; Burguete, D.; Li, H.; Huet, G.; Yuan, Q.; Wigal, T.; Butt, Y.; Ni, M.; Torrealba, J.; Oliver, D.; Lenkinski, R. E.; Malloy, C. R.; Wachsmann, J. W.; Young, J. D.; Kernstine, K.; DeBerardinis, R. J. *Cell* **2017**, *171*, 358−371. e9.
(17) Maher, E. A.; Marin-Valencia, I.; Bachoo, R. M.; Mashimo, T.; Raisanen, J.; Hatanpaa, K. J.; Jindal, A.; Jeffrey, F. M.; Choi, C.; Madden, C.; Mathews, D.; Pascual, J. M.; Mickey, B. E.; Malloy, C. R.; Deberardinis, R. J. *NMR Biomed.* **2012**, *25*, 1234−1244.
(18) Johnson, A. S.; Crandall, H.; Dahlman, K.; Kelley, M. C. *J. Am. Coll. Surg.* **2015**, *220*, 581−593. e1.
(19) Antoniewicz, M. R.; Kelleher, J. K.; Stephanopoulos, G. *Metab. Eng.* **2007**, *9*, 68−86.
(20) Weitzel, M.; Nöh, K.; Dalman, T.; Niedenführ, S.; Stute, B.; Wiechert, W. *Bioinformatics* **2013**, *29*, 143−145.
(21) Klein, S.; Heinzle, E. *Wiley Interdiscip. Rev. Syst. Biol. Med.* **2012**, *4*, 261−272.
(22) Antoniewicz, M. R. *J. Ind. Microbiol. Biotechnol.* **2015**, *42*, 317−325.
(23) Wittmann, C. *Adv. Biochem. Eng. Biotechnol.* **2002**, *74*, 39−64.
(24) Niedenführ, S.; ten Pierick, A.; van Dam, P. T. N.; Suarez-Mendez, C. A.; Nöh, K.; Wahl, S. A. *Biotechnol. Bioeng.* **2016**, *113*, 1137−1147.
(25) Rühl, M.; Rupp, B.; Nöh, K.; Wiechert, W.; Sauer, U.; Zamboni, N. *Biotechnol. Bioeng.* **2012**, *109*, 763−771.
(26) Wu, L.; Mashego, M. R.; Van Dam, J. C.; Proell, A. M.; Vinke, J. L.; Ras, C.; Van Winden, W. A.; Van Gulik, W. M.; Heijnen, J. J. *Anal. Biochem.* **2005**, *336*, 164−171.
(27) Dzeletovic, S.; Breuer, O.; Lund, E.; Diczfalusy, U. *Anal. Biochem.* **1995**, *225*, 73−80.
(28) Baillie, T. A. *Pharmacol. Rev.* **1981**, *33*, 81−132.
(29) Kombu, R. S.; Brunengraber, H.; Puchowicz, M. A. Analysis of the Citric Acid Cycle Intermediates Using Gas Chromatography-Mass Spectrometry. In *Metabolic Profiling*; Humana Press, 2011.

(30) Heuillet, M.; Millard, P.; Cissé, M. Y.; Linares, L. K.; Létisse, F.; Manié, S.; Le Cam, L.; Portais, J. C.; Bellvert, F. *Anal. Chem.* **2020**, *92*, 5890−5896.
(31) Bligh, E. G.; Dyer, W. J. *Can. J. Biochem. Physiol.* **1959**, *37*, 911−917.
(32) Wahl, S. A.; Dauner, M.; Wiechert, W. *Biotechnol. Bioeng.* **2004**, *85*, 259−268.
(33) Wood, P. L.; Khan, M. A.; Moskal, J. R. *J. Chromatogr. B: Anal. Technol. Biomed. Life Sci.* **2006**, *831*, 313−319.
(34) Mawhinney, T. P.; Robinett, R. S. R.; Atalay, A.; Madson, M. A. *J. Chromatogr. A* **1986**, *358*, 231−242.
(35) Frederick Schwenk, W.; Berg, P. J.; Beaufrere, B.; Miles, J. M.; Haymond, M. W. *Anal. Biochem.* **1984**, *141*, 101−109.
(36) Yang, L.; Kasumov, T.; Yu, L.; Jobbins, K. A.; David, F.; Previs, S. F.; Kelleher, J. K.; Brunengraber, H. *Metabolomics* **2006**, *2*, 85−94.
(37) Moore, S.; Spackman, D. H.; Stein, W. H. *Anal. Chem.* **1958**, *30*, 1185−1190.
(38) Stacpoole, P. W. *Metabolism* **1989**, *38*, 1124−1144.
(39) Abildgaard, C.; Dahl, C.; Basse, A. L.; Ma, T.; Guldberg, P. *J. Transl. Med.* **2014**, *12*, No. 247.
(40) Sun, R. C.; Fadia, M.; Dahlstrom, J. E.; Parish, C. R.; Board, P. G.; Blackburn, A. C. *Breast Cancer Res. Treat.* **2010**, *120*, 253−260.
(41) Kankotia, S.; Stacpoole, P. W. *Biochim. Biophys. Acta, Rev. Cancer* **2014**, *1846*, 617−629.
(42) Goodman, M. N.; Ruderman, N. B.; Aoki, T. T. *Diabetes* **1978**, *27*, 1065−1074.
(43) Bowker-Kinley, M.; Davis, W. I.; Wu, P.; Harris, R.; Popov, K. *Biochem. J.* **1998**, *329*, 191−196.

https://doi.org/10.1021/acs.analchem.1c01040
Anal. Chem. 2021, 93, 8248−8256